Energy Equip. Sys./ Vol. 8/No. 1/March 2020/ 1-22

ENERGY EQUIPSYS

Energy Equipment and Systems

http://energyequipsys.ut.ac.ir
www.energyequipsys.com

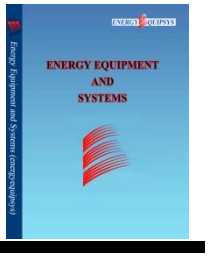

Design and optimization of an energy hub based on combined cycle power plant to improve economic and exergy objectives

Authors

Mostafa Mostafavi Sani [a]
Alireza Noorpoor [a*]
Majid Shafie-Pour Motlagh [a]

[a] Graduate Faculty of Environment, College of Engineering, University of Tehran, Tehran, Iran

Article history:

Received : 21 December 2018
Accepted : 5 March 2019

ABSTRACT

This paper uses the energy hub concept to meet the water, heat and electricity demand of a power plant in the Qeshm island in south of Iran. Given the power plant's high potential for waste heat recovery and some scenarios were considered using the hub energy concept based on energy, exergy, environmental and economic analyzes in terms of meeting the demands of the hub and purchasing/selling energy carriers including electricity, heating, freshwater as well as its production using gas turbine, steam turbine, boiler, Reverse Osmosis (RO) and Multi-Effect Desalination (MED) system. Energy hubs are optimized based on the Genetic Algorithm (GA) with the goal of supplying demand, as well as reducing costs and pollutants and increasing the exergy efficiency which ultimately will be selected using the concept of an energy hub at its optimal capacity. By comparing the two energy supplying systems of the current case study and optimal energy hub, results showed that the Total Annual Cost (TAC) level decreased by about 257904 $/year and exergy efficiency increased by 34.31%. CO_2 emission will also decrease by about 471 tons/year.

Keywords: Energy hub; Multi-Effect Desalination (MED); Reverse Osmosis (RO); Total Annual Cost (TAC); Genetic Algorithm.

1. Introduction

Given that fifty-nine percent of drinking water is supplied from the sea through desalination processes [1], different methods have been developed for the production of freshwater from the sea across the world. Energy expenditure (thermal, electricity) in water desalination systems are as follows: RO<MED<MSF (Multi-stage flash distillation) [1-3]. From the years 2013 to 2014, 77.4 million cubic meters of desalinated water was produced, of which 65% was produced for the RO system [1].

Between the years 2015 to 2017, 3.7 million cubic meters were added to this capacity [4, 5]. 40% to 50% of the main energy expenditure for the RO system is relevant to the operating system [2, 6]. The energy used for RO system is dependent on the salinity of the water as well as the system used for energy recovery. For seawater, the energy consumption with and without the recycling device is 12 and 4 kWh/m^3, respectively. However, with the development and improved performance of RO systems, the price of desalinated water has decreased from 2 \$/m^3 to roughly 0.8 \$/m^3[1, 7]. However, the MED thermal water desalination system is still developing and has retained its position across the world. MED system has a heating

* Corresponding author: Alireza Noorpoor
Graduate Faculty of Environment, College of Engineering, University of Tehran, Tehran, Iran
Email: noorpoor@ut.ac.ir

energy consumption of 71.7 kWh and electricity consumption of 2.3 kWh [8]. The existence of rich oil and gas resources in the Middle East as well as the use of heat waste has led to the installation of such systems at various capacities. Energy consumption for phase change in these systems is 2330 kJ/kg [9].

Considering the high energy consumption of water desalination systems as well as rising fresh water demand (from 77.4 in 2014 to 92 million in 2018), this technology has become a major source of CO_2 emissions [8]. In this regard, CO_2 production is estimated at 100 million tons per year [1, 8]. In other words, for each cubic meter of fresh water, about 3 kg of greenhouse gas is generated [10, 11], and about 10,000 tons of oil is needed annually to produce 1,000 fresh water in cubic meters per day [12]. The increasing trend in 2040 will bring greenhouse gas emissions to 218 tons per year and an approximate temperature increase of 2 °C [9, 13, and 14]. Because of potable water production in sunny and remote regions, there is a new method where primary energy is provided by solar energy. This method the extensive scale application of typical water desalination methods is faced with several political, economic and technological obstacles. Such methods are not implemented in decentralized areas which have weak infrastructure because of a constant requirement of electricity supply and qualified maintenance [15, 16].

Due to the high energy consumption of RO and MED, in order to 1) reduce costs 2) reduce greenhouse gas production 3) increase productivity and 4) reduce gas and oil consumption in energy rich areas (such as the Persian Gulf), heat waste from factories can be used to produce desalinated water and meet regional demands (power generation and water heating). The existence of rich gas and oil resources has led to industrial development in this region. Also, population dispersion in the Persian Gulf due to climatic conditions as well as the existence of various islands in the area has become an issue for governments to meet the existing energy demand of residents. In regard to the water production along with other energy requirements is an energy-intensive process, it is logical to define an energy hub. The point of confrontation energy carriers, conversion equipment, energy storage and energy demand is known as the energy hub. Energy hub utilization will lead to 1) reduction in energy consumption 2) simplicity and high accuracy in multiple system carrier analysis and assessment 3) increased reliability 4) multi-dimensional analysis of energy systems (technical, economic, environmental). The main element in defining energy networks is the energy hub. Numerous researches have been conducted on the hub. A residential energy hub model was proposed by Brahman et al. [17] that obtains solar radiation, natural gas (NG) and electricity as inputs to provide cooling, heating and electricity at its output port. An optimization issue was dealt with regarding the management of electrical and thermal energy with the aim of reducing total energy costs of customer's input in terms of NO_x, CO_2 and SO_x emissions. Mohammadi et al. [18] addressed the advantages of integrating options such as smart technologies, storage systems, multi-generation systems, renewable energy resources, demand side management and distributed energy resources by proposing the smart energy hubs concept. In order to utilize renewable sources with zero emissions into dispatchable combined cycle power plants, AIRafea et al. [19] presented a modern energy hub. For this energy hub, hydrogen is introduced as an energy vector to replace coal fired Nanticoke power plant. With the addition of hydrogen into natural gases as a combined cycle power plant's fuel, additional annual revenue reduction and costs will be the consequences. CO_2 and NO_x emission credits will also increase. In order to start increasing annual revenue, electricity should be sold at 0.12 $ per kWh with hydrogen at 3.7% in fuel of CCPP. To maximize the employment of waste heat from coal fired plants for the benefit of factories in the vicinity, Togawa et al. [20] proposed a stimulation process model that integrates land use control, technology systems and spatial analysis. The acquired results showed that waste heat systems exhibited several environmental advantages compared to the individual boiler systems. By employing waste heat, the consumption of fuel oil is reduced by 16.05 TJ per year and there is a CO_2 emissions reduction of 1204 ton/year.

Another solution to reduce energy consumption and environmental consequences is to use heat waste from

factories and to implement a comprehensive integrated system in remote areas suffering from water shortages. This paper addresses heat from a power plant. Iran is one of the largest power plant based on natural gas around the world [21-24]. In the case of integrated systems and the use of heat waste, the work of Salimi and Amidpour [25] can be referred to, which, based on the R-curve, examined the integration of different water desalination systems. The results of this study showed that according to the system characteristic and its functional point before or after the optimum point in the R-Curve, the addition of each of the RO and MED systems through the use of electric and thermal energy (In order) is effective in improving the overall system status. Chiranjeevi and T.Srinivas [26] investigated the integrated system for a solar steam plant, in which the MED system is placed to recover the heat that previously wasted by condenser. This research has been carried out for a mine requiring desalinated water to simultaneously produce water and electricity. Marco Astolfi et al. [27] utilized solar energy on a small island to increase system sustainability for the production of desalinated water. This section assesses a photovoltaic and centralized control system along with an organic Rankine cycle for the RO and MED systems. The results of this integration led to the reduction of fuel consumption and are economically more feasible compared to current methods. Mokhtari et al. [28] proposed the GT+MED+RO water desalination method based on exergy and thermo-economics analysis for the Persian Gulf region. The system was designed on the basis of the simultaneous generation of electricity and water and could reduce total water production costs. Muhammad Wakil Shahzad et al. [29] proposed a combination of absorption and RO systems based on low temperature industrial heat sources or heat from sun to address lack of water in the Persian Gulf region, which resulted in 81% efficiency and energy consumption of 1.76 kWh/m^3. Azhar et al. [30] produced power, desalinated water and provided cooling as an integrated system based on a solar cycle connected to a Rankine cycle. This system functions based on industrial heat, solar energy, geothermal energy and ocean thermals. Arash Nemati et al. [31] utilized heat waste from a large diesel ship engine to produce desalinated seawater. On the basis of the radiation curve amidst optimization, the obtained efficiency was 37% and the cost of exergy destruction was 60 $/GJ. Reynolds et al. [32] suggested a district energy management optimization strategy for the optimization of district heat generated from a multi vector energy center. In this study, the variables such as building demand are predicted in order to utilize using a Genetic Algorithm to ascertain optimal operating schedules of thermal storage, heating set point temperature and heat generation equipment. The outcomes show the possible gain when energy is managed in a holistic state, taking both supply and demand into account as well as multiple energy vectors.

By assessing various papers on energy hubs and separating the subject areas of these papers, it is clear that there are limited assessments on heat energy carrier, electricity and water that are subject to energy, exergy and environmental analyzes. In addition, most papers have addressed energy hub system optimization in a single-objective manner. Also, in all papers the coupling matrix conversion factor is considered constant. In this paper, by using the coupling matrix parameters such as efficiencies, recoveries and GOR are included variables. Hence, not only energy flow will be optimized, but the coupling matrix conversion factor and components capacities within the hub will be determined by considering design parameters. For example, in the MED model, the final value obtained for GOR in the coupling matrix is related to the temperature and hot water inlet. Moreover, this paper addresses thermal loss in electricity, heat and fresh water production based on energy, exergy, economic and environmental analyzes in a case study. In the desalination system, both commonly used MED and RO systems are implemented. To produce fresh water, these two systems require heat and electricity, respectively.

Some of the main novelties of this paper are:

- Considering water as an energy carrier in the concept of energy hub;
- Using two kinds of desalination systems (MED and RO) for the production of pure water from various sources of electricity and heat, simultaneously;

- Taking into account variable coupling matrix factors (relative to the design parameters of each component) in order to increase accuracy of dispatch factors as well as the operational model of the system;
- Two objectives optimization of the power plant energy hub by considering exergy, economic and environmental analysis.

In this paper, an energy hub simulation model is presented. The main energy sources include CHP as the main energy source (both heat and electricity), steam turbine and boiler back up. For potable water production, the hub uses RO and MED. Power and heat can be utilized in other consumer destinations as energy carriers. Thus, the objective of this research is to create a simulated model which combines various energy generation methods that will be examined in terms of produced emissions, cost per year of energy generated and total energy production. The developed model assesses the advantages of energy hubs, in addition to environmental, energy, economic and technological obstacles by presenting numerous scenarios. MATLAB software was used to simulate the mentioned scenarios. Ten design parameters were considered which consisted of RO water dispatch factors, steam turbine power, backup boiler heat, MED water, GT (CHP unit power), boiler maximum heat, power consumption per water desalinated, MED hot water flow rate, MED hot water inlet temperature and active recovery rate. Non dominated elitist and rapid Sorting Genetic Algorithm (NSGA-II) was implemented to present a series of Pareto multiple optimal solutions.

Nomenclature

List of acronyms

CCPP	Combined-Cycle Power Plant
CHP	Combined Heat and Power
CRF	Capital Recovery Factor
CTGs	Combustion Turbine Generators
EW	Energy consumption per Water production in RO
GOR	Gained Output Ratio
GT	Gas Turbine
LHV	Lower Heat Value (kJ/kg)
MED	Multi-Effect Desalination
NSGA	Non dominated elitist and rapid Sorting Genetic Algorithm
NG	Natural Gas
MSF	Multi-stage flash distillation
SDI	Silt Density Index
TAC	Total Annual Cost ($/year)
WHO	World Health Organization

List of symbols

C_{ij}	Coupling matrix
C_w	Brine concentration [kg/m^3]
CC	RO capital cost subsystems
d_i	Distance from the ideal point
D_s	Solute diffusivity [m^2/s]
e, ex	Exergy (kJ/kg)
Ex	Exergy flow (kW)
T_{hot}	Hot water temperatures (˚ C)
v	Dispatch factors (-)
$\dot{Z}$	Capital cost rate ($/year)
Z_k	Component purchase cost ($)
$Z_{O\&M}$	Operation and Maintenance Cost

Subscripts

amb	Ambient
b	Boiler and brine
bp	Brine Pump
CC	Combustion Chamber
ch	Chemical
CV	Control Volume
D	Distraction
dmn	Demand
e	Exergy
hot	Hot water
hpp	High Pressure Pump
m	Material/Membrane
max $_{Boiler}$	Maximum Boiler
NG	Natural Gas
P	Pump
pipeline	Pipe line
Ph	Physical
Q	Heat
EW_{RO}	Electrical consumption per water production
F_{ij}	Non-dimensionalize objective indexes

f_m	Material correction factor
K	Mass transfer coefficient [m/s]
L	Output loads of the hub
LD_e	Output electrical loads of the hub (kW)
LD_h	Output heat loads of the hub (kW)
LD_w	Output water loads of the hub (kW)
N	Operation hours in a year
m_f	Feed water flow rate (kg/s)
m_{hot}	Hot water flow rate (L/s)
P	Input carriers of the hub
P_E	Exchanging electricity of the hub (kW)
P_H	Exchanging heat of the hub (kW)
P_W	Exchanging water of the hub (kW)
P_i	Hub input vector
P_j	Hub output vector
Q	Heat flow (kW)
R_{RO}	Recovery (%)
Re	Reynolds number
S	Sell
ST	Steam Turbine
SW	Sea Water
W	Water
w	Membrane wall
i	Interest rate
0	Standard Situation

Greek symbols

$\alpha,\beta,\omega,\varepsilon$	Type of energy carrier
η	Efficiency
ρ	Density (kg/ m^3), Integer Numbers
ξ	Chemical exergy/energy ratio
ε	Total cycle exergy efficiency (-)
τ	Operation hours per year (h)
φ_f	Fuel cost ($/kg)
$\varphi_{e,s}$	Selling electricity cost ($/kWh)
ρ_p	Density of the permeate [kg/m^3]
π	Osmotic pressure [MPa]
$\varphi_{e,b}$	Buying electricity cost ($/kWh)
ψ_{em}	Pollutant emission cost ($/kg)

2. Thermal modeling

2.1. Energy Hub

Increased environmental concerns, the lack of fossil fuels, and the unlimited increase of demand, coupled with the progress of powerful multi-generation systems entails the utilization of existing energy structures. Efficient utilization of these systems wants a management of integrated energy system for optimal control. The energy hub is a new and promising concept to optimally manage multiple energy carrier systems. The energy hub has undoubted potential for realizing energy system models and moves towards sustainable multi-energy system [18, 36]. In order to achieve an integrated system, a modeling and analysis framework for multi-carrier energy systems must be developed. The current model is between converter devices based on the efficiency of the output-to-input ratio. When there are numerous outputs, a coupling or conversion matrix is defined that represents the transformation of energy carriers from the input to the hub outputs. If necessary, storage devices are used that take time and energy into account [37]. The energy conversion between different energy hub ports is typically shown using a coupling matrix (C). The relationship between different input and output ports for an example hub is shown in Fig. 1.

The exchangeable power in i and j ports are expressed by P_i and P_j vectors respectively and these power vectors are related via the coupling matrix by the following equations. In this equation, the C_{ij} is the coupling matrix array which; according to the characteristics of the existing elements, associate the hub inputs and outputs (Eq. (1)) [37].

$$\underbrace{\begin{bmatrix} P_j^{\alpha} \\ \vdots \\ P_j^{\omega} \end{bmatrix}}_{P_i} + \underbrace{\begin{bmatrix} C_{ij}^{\alpha\alpha} & \cdots & C_{ij}^{\omega a} \\ \vdots & \ddots & \vdots \\ C_{ij}^{\alpha\omega} & \cdots & C_{ij}^{\omega\omega} \end{bmatrix}}_{C_{ij}} \underbrace{\begin{bmatrix} P_i^{\alpha} \\ \vdots \\ P_i^{\omega} \end{bmatrix}}_{P_i} = 0 \qquad (1)$$

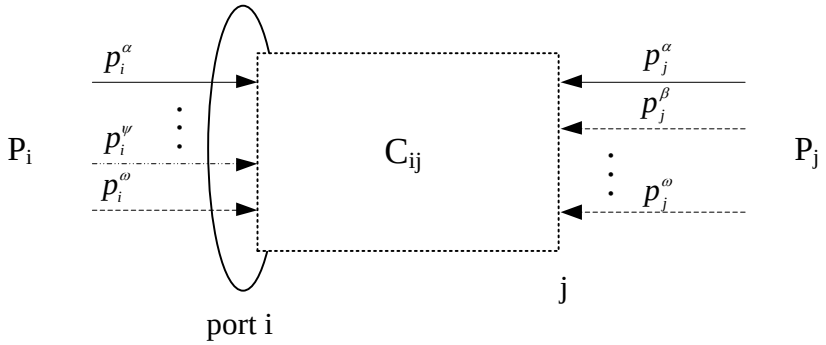

Fig. 1. Relationship between the input and output ports of an energy hub with a Cij coupling matrix [49]

There are two important properties in the coupling matrix arrays:

1- According to the energy conservation law, energy is not converted from one form to another, but in the process of conversion, there is also some energy wasted, so all coupling matrix arrays fall into the maximum or minimum values according to the following equation (Eq. (2)) [37].

$$0 \le C_{ij}^{\alpha\beta} \le 1 \qquad \forall(i,j)\epsilon\rho \quad \text{and} \quad \alpha,\beta \epsilon \varepsilon \tag{2}$$

In this equation:

$$\forall(i,j)\ \epsilon\ \rho = \{(1,2),(3,4),\dots\}, \alpha,\beta,\omega \epsilon \varepsilon = \{Heating, Cooling, Electrical, Water\} \tag{3}$$

2- According to the total energy conservation law, all outputs converted from a given input must be less than or equal to the input value. Therefore, the total arrays of each column in the coupling matrix must be less than or equal to the relation below (Eq. (4)) [37].

$$0 \le \sum_{\beta\epsilon\varepsilon} C_{ij}^{\alpha\beta} \le 1 \qquad \forall(i,j)\epsilon\rho \quad \text{and} \quad \alpha,\beta \epsilon \varepsilon \tag{4}$$

If the output loads of the hub are represented by L and the input carriers of the hub are represented by P, the previous equation can be rewritten as follows:

$$\underbrace{\begin{bmatrix} L_\alpha \\ \vdots \\ L_\omega \end{bmatrix}}_{L} = \underbrace{\begin{bmatrix} C_{\alpha\alpha} & \cdots & C_{\omega\alpha} \\ \vdots & \ddots & \vdots \\ C_{\alpha\omega} & \cdots & C_{\omega\omega} \end{bmatrix}}_{C} \underbrace{\begin{bmatrix} P_\alpha \\ \vdots \\ P_\omega \end{bmatrix}}_{P} \tag{5}$$

As long as the coupling matrix elements, known as an efficiency of energy hub equipment, have a constant and independent values, Eq. (5) is linear. However, considering the dependence of the equipment efficiency on the input energy, this equation will be nonlinear [37].

Since one type of input energy into the hub may be split into several parts and enters various converters within the hub, coefficients named dispatch factors are defined which represent the amount of input energy assigned to each of the hub convertors. In multi-output and multi-input hubs, the number of coupling matrix elements depends on the dispatch factors as well as the converter equipment efficiency. Figure 2 shows the industrial plant configuration evaluation for this section. Commercially available water oriented industry technology is the basis of this design. This plant consists of a MED for potable water production, RO plant, steam turbine, and combustion turbine generators (CTGs) and a boiler. The plant scope is identified and specified according to the aim of this research and multigenerational factors. An alternative energy source and high efficiency are proven properties of this plant to minimize CO_2 emissions.

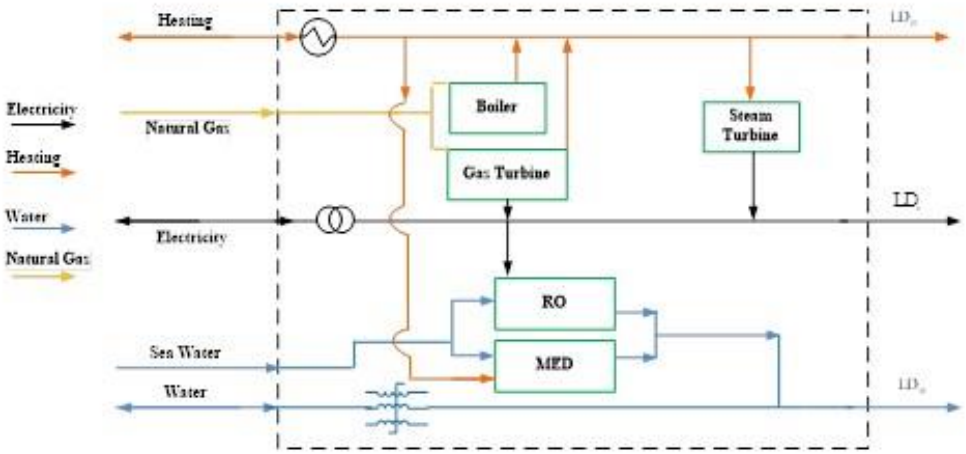

Fig. 2. Schematic view of energy hub used in case study

Figure 2 presents thermal plant overall system flow. Three varying potential energy sources were taken into account. Heat waste in gas turbine was the first source. The second source was exhausted gas from the GT stack. The third source was heat energy from the boiler. Electrical load requirements for the energy hub can be met using energy sources such as electrical grid, steam turbine, and GT systems. The dispatch factors v_{MED}, v_{Boiler}, v_{CHP}, v_{ST} and v_{RO} are in interval at all times [0, 1]. As previously stated, the energy hub model is considered for multi-energy carrier systems and represents continuity equations by considering a control volume such that each input energy carrier to the system is multiplied by the coupling matrix coefficient, exhibiting its influence on the considered output load so that the sum of these inputs determines the output load by taking the energy hub productions and consumptions into account. The important point is that the output loads are known as specified quantity in each energy hub which ultimately, by expanding the equations (Table 1) and implementing decision variables and assumptions for each equipment and energy converters, the required input energy to the system, the coupling matrix coefficients, and hence the capacities of each equipment can be determined. The decision variables for each equipment and dispatch factors are related to the considered objective function in optimization and will be determined accordingly. Thermal, electrical and water loads shown as LD_H, LD_e and LD_W respectively. Section 7 shows decision parameter values, v_{MED}, v_{Boiler}, v_{ST}, v_{RO}, R_{RO}, T_{hot}, M_{hot}, EW_{RO}, $Q_{max,Boiler}$ which are determined by the GA optimization method given their limits. The values of GT efficiency (η_{CHP}) and steam cycle efficiency (η_{ST}) are obtained according to the reference curve of the power plant characteristics. The GOR value will also be determined from section 2.3 from the T_{hot} and M_{hot} decision variables. According to Table 1, 12 variables can be determined from 12 equations and the energy hub can be obtained.

In Table 1, row 1 of the energy continuity equation for electric current is presented in Fig. 2. In GT power generators and steam turbines, these inputs should be equal to electrical consumption of RO and the power consumption of the hub. Rows 2 and 3 are auxiliary equations that are extracted according to their definition. In row 4 of this table, the hub water affinity equation is presented. The water produced by the RO and MED system should be equal to the demand for water. In row 7, the heat produced by the GT, boiler and heat waste from the gas turbine are heat generators in the hub, which should provide the heat required by the steam turbine, MED and hub thermal demand. Also, the current (P_E), water (P_{SW}) and heat (P_H) input to the hub from the grid or the output from the hub to the grid can be placed with a positive and negative sign respectively. All equations of rows 2, 3, 4, 5, 6, and 8 are defined by dispatch factors v_{CHP}, v_{ST}, v_{RO}, v_{MED}

Table 1. Design equation for energy hub model [20]

Row	Equations	Unspecified quantity	Specified quantity	Decision variables
1	$Pe_{CHP} + Pe_{ST} + P_E - Pe_{RO} - LD_e = 0$	$Pe_{CHP}, Pe_{ST}, P_E, Pe_{RO}$	LD_e	
2	$Pe_{CHP} = v_{CHP}(Pe_{ST} + P_E - Pe_{RO})$			v_{CHP}
3	$Pe_{ST} = v_{ST}(Pe_{CHP} + P_E - Pe_{RO})$			v_{ST}
4	$m_{RO} + m_{MED} + P_{SW} - LD_w = 0$	m_{RO}, m_{MED}, P_{SW}	LD_w	
5	$m_{RO} = v_{RO}(m_{MED} + P_{SW})$			v_{RO}
6	$m_{RO} = v_{MED}(m_{RO} + P_{SW})$			v_{MED}
7	$Q_{CHP} - Q_{ST} + Q_b + P_H - Q_{MED} - LD_H = 0$	$Q_{CHP}, Q_{ST}, Q_b, P_H$	LD_H	
8	$Q_b = v_{Boi}(Q_{CHP} - Q_{ST} + P_H - Q_{MED})$			v_{Boi}
9	$Pe_{RO} = EW_{RO} m_{RO}$			EW_{RO}
10	$Q_{CHP} = \frac{(1-\eta_{CHP})}{\eta_{CHP}} Pe_{CHP}$		η_{CHP}	
11	$Q_{ST} = \frac{Pe_{ST}}{\eta_{ST}}$		η_{ST}	
12	$GOR = \frac{m_{MED}}{Q_{MED}} \frac{2326\ kj}{1\ kg}$		GOR	

and v_{Boi} which are decision variables and determine the amount of energy distribution in each of the energy carriers within the hub equipment.

2.2. RO modeling

Two modeling methods for the RO system are proposed by FILMTEC [39]. The first method is element to element. In the second method, if the feed quality, temperature, and intensity of the purified water flow and the number of elements are known, the average value is used to calculate the feed pressure and quality of purified water. If, instead of the number of elements, the feed pressure is specified, the number of elements is obtained through several integration equations. The design equations for the FILMTEC SW30 8-inch elements are given in the references [39]. In this paper, considering the demand for water and the maximum water quality required based on the World Health Organization (WHO) standard for drinking water [40], the required water recovery, 6 elements per pressure vessel, membrane type selection (SW30XLE-400i) and water flow intensity and a silt density index (SDI) of under 3 [39], and the amount of power assigned to the RO can be determined based on the amount of feed pressure. The mean value method is considered. In regard to the hub, by determining the amount of power, the pressure can be determined based on the equation below [39].

$$\dot{W}_P = \frac{\dot{m}_f (P_f - P_{amb})}{\rho \eta_P} \quad (6)$$

In Eq. (6), P_f is feed stream pressure; P_{amb} is ambient pressure; η_P is pump isentropic efficiency and ρ is water density.

In this model, the Pelton turbine has been used as an energy recovery system. According to Eq. (7), the amount of energy required by the RO system can be determined in accordance to Eq. (8) [39]. In Eq. (7), P_b is pressure of brine stream and P_p is pressure of permeate stream.

$$\dot{W}_T = \frac{\dot{m}_b (P_b - P_p)}{\rho_{out}\, \eta_T} \quad (7)$$

$$\dot{W}_{net} = \dot{W}_P - \dot{W}_T \quad (8)$$

2.3. MED modeling

According to reference [38] where a multi-effect distillation system is assessed as experimental characterization, a number of empirical equations are extracted in order to measure the performance of the system under

off-design conditions. In addition, the impact of the key parameters variation where the MED plant is determined (inlet hot water temperature (T_{hot}) and flow rate (m_{hot})) on GOR and freshwater production were evaluated with an empirical campaign of 82 tests. The MED plant steady state results working at off-design circumstances are addressed in a state which presents: The T_{hot} and the m_{hot} effect on the production of distillate (m_{MED}) and on the plant GOR. The MED modeling equations are presented in this section. Eq. (9) and Eq. (10) are valid for $60 \leq T_{hot} \leq 74$ ℃ and $7 \leq m_{hot} \leq 14\ \frac{L}{S}$ [38].

$$m_{MED} = -0.273 + (0.008409\ T_{hot}) - (0.04452\ m_{hot}) + (0.0003093\ T_{hot}^2) - (0.002485\ m_{hot}^2) + (0.001969\ T_{hot}\ \ m_{hot}) \quad (9)$$

$$GOR_{MED} = 648.2 - (26.74\ T_{hot}) - (16.45\ m_{hot}) + (0.3842\ T_{hot}^2) + (0.3137\ T_{hot}\ \ m_{hot}) + (0.5995\ m_{hot}^2) - (0.001835\ T_{hot}^3) - (0.002371\ T_{hot}^2\ \ m_{hot}) - (0.01844\ m_{hot}^3) - (0.0001411\ T_{hot}\ m_{hot}^2) \quad (10)$$

The final parameter finds out the MED plant thermal efficiency (GOR) and it is shown in Table 1. (Row 12). Where m_{MED} is the distillate production (L/s); Gain origin ration (GOR) (-); hot water temperatures (T_{hot}), and the hot water flow rate (m_{hot}); Q_{hot} Heat consumed by MED.

Parametric equations were successfully achieved in reference [38] prior to being statistically validated to predict the GOR and distillation production as a function of various input parameters via an extensive validation range.

3. Exergy analysis

Exergy analysis can aid in developing planning and measures for the effective use of energy in various systems. Exergy can be divided into four classes. Two prominent types of exergy are physical exergy and chemical exergy. In this study, kinetic and potential exergy are hypothesized as negligible. The physical exergy equals the maximum workable flow of matter and is determined by a process from the initial state or an environment that only involves heat exchange with its surroundings. The maximum work acquired when each substance concentration in the system varies to its concentration in the ambient at the ambient temperature and pressure (T0, p0) is the chemical exergy. It is prominent to note that the chemical exergy will ignore if the environment and the system are both pure substances (for example: pure water). Even so, for a multi-component system (for instance: exhaust gases and seawater) the chemical exergy should be assessed. By using the first and second law of thermodynamics, the following exergy equilibrium is obtained [41-44].

$$\dot{Ex}_Q + \sum_i \dot{m}_\iota\ ex_i = \sum_e \dot{m}_e\ ex_e + \dot{Ex}_W + \dot{Ex}_D \quad (11)$$

The χ parameter indicates that when exergy flow is outside the control volume shown in Fig. 3 and enters the system (χ=Buy), it is considered positive in equations and if exergy flow exits volume control (χ=Cell) it is shown as negative in equations. In Fig. 3, exergy flow is calculated as:

$$\dot{Ex}_{NG} = \dot{m}_{f,Total}\ LHV\ \xi \quad (12)$$

where parameter ξ is defined as follows for NG [42]:

$$\xi = 1.03 + 0.017\ \frac{y}{x} - \frac{0.07}{x} \quad (13)$$

Water flow exergy is equal to [45]:

$$\dot{Ex}_{Water} = \dot{Ex}_{Water}^{ch} + \dot{Ex}_{Water}^{ph} \quad (14)$$

where $\dot{Ex}_{Water}^{ch}$ and $\dot{Ex}_{Water}^{ph}$ are water physical exergy and chemical exergy respectively and are calculated in [45]. For an ideal mixture model of seawater, the chemical exergy is determined as [45].

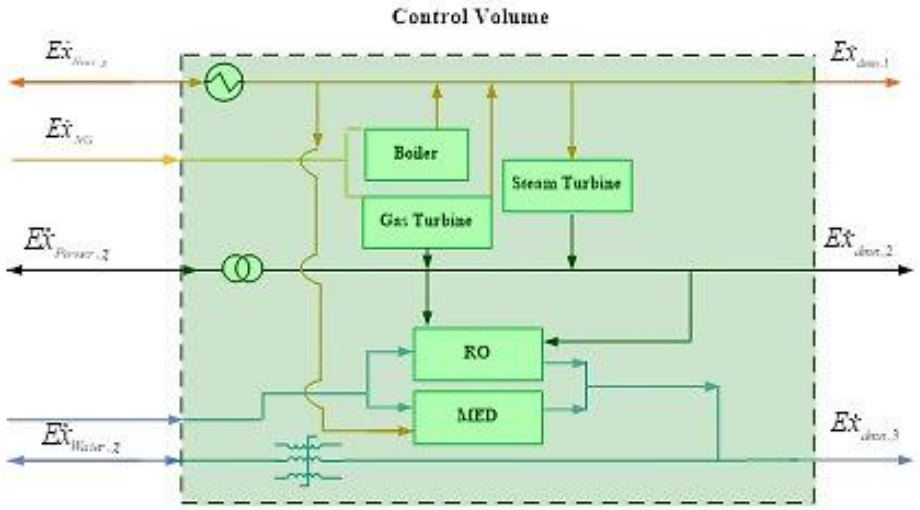

Fig. 3. Schematic view of exergy hub flow

$$e = \sum_{j=1}^{m} w_j R_j T \ln\left(\frac{y_j}{y_{j,0}}\right) \quad (15)$$

In which $y_{j,0}$ is evaluated at a hypothetical standard state, y_j is the mole fraction and w_j is mass fraction for the component j. Heat exergy and electricity are calculated based on Eq. (16) and Eq. (17) [46]:

$$\dot{E}x_Q = \left(1 - \frac{T_o}{T_i}\right)\dot{Q}_i \quad (16)$$

$$\dot{E}x_{Power} = \dot{W} \quad (17)$$

In Eq. (16) the term Q_i shows the heat transfer time rate at the energy hub boundary in which the T_i is the absolute temperature of the heat source and T_0 refer to the ambient conditions. Finally, hub exergy efficiency is calculated based on Eq. (18) [46]:

$$\varepsilon = \frac{\sum_{t=1}^{N} \dot{E}x_{p,t}}{\sum_{t=1}^{N} \dot{E}x_{f,t}} = \frac{\sum_{t=1}^{N}\left(\sum_{i=1}^{3} Ex_{dmn,i}\right)\tau_t}{\sum_{t=1}^{N}\left(\dot{m}_{f,CHP}\, LHV + E_b\right)\tau_t} \quad (18)$$

If i=1, heat exergy of the demand heat flow is calculated as follows [60]:

$$\dot{E}_{dmn,1} = \left(1 - \frac{T_0}{T_h}\right)\dot{H}_{dmn} \quad (19)$$

If i=2, electricity demand exergy is calculated as follows [46]:

$$\dot{E}_{dmn,2} = \dot{E}_s \quad (20)$$

If i=3, water demand exergy is calculated as follows [45]:

$$\dot{E}_{dmn,3} = \dot{E}_{Water} = \dot{m}_{water}\dot{E}x^{dmn}_{water} \quad (21)$$

4. Economic analysis

Economic analysis is required to select equipment and coefficients stated in the hub section. In economic analysis, equipment costs and maintenance costs are calculated according to the utilized equipment. Eq. (22) is used to estimate MED costs [60]:

$$C_{MED} = Z_{MED} CRF + Z_{O\&M} \quad (22)$$

$Z_{O\&M}$ is calculated by Eq. (23) [10].

$$Z_{MED} = C\ \dot{m}_{Fresh\ water} \quad (23)$$

In this equation, C = 81430.27 $ according the reference [48]. Other hub costs are set according to Table 1. Economic parameters are determined based on reference [49, 50] shown in Table 2. The cost of the transmission line is also determined by Eq. (24) with unit of $/m [20].

$$C_{Pipeline} = 0.9734\ (32000 + 213000\ D) \quad (24)$$

In which D is the media pipe diameter (m). Finally, TAC is calculated based on Eq. (25) [51]:

Table 2. The cost functions for each equipment of energy hub [49, 50].

Component	Cost function
GT	$Z_{GT} = (-0.014\ P_{GT} + 600)P_{GT}$
Steam Turbine	$Z_{ST} = 1200\ P_{ST}$
Boiler	$Z_{Boiler} = 205\dot{Q}_{Boiler}^{0.87}$

$$\begin{aligned} &TAC\ \left(\$/_{year}\right) \\ &= C_{MED} + C_{RO} + C_{GT} + C_{ST} + C_B \\ &+ C_T \\ &+ \sum_{t=1}^{N}\left[E_b\varphi_{e,b} - E_s\varphi_{e,s}\right. \\ &+ \dot{m}_{f,total}LHV_{fuel}\varphi_f \\ &\left.+ 3600\ m_{co2}\psi_{em}\right]\tau \end{aligned} \quad (25)$$

Table 3 presents cost parameters. τ is an hour time period and N is equal to 8760 hours. Capital recovery factor (CRF) is dependent on equipment estimated life and interest rates and is written as [60]:

$$CRF = \frac{i\ (1+i)^{year}}{(1+i)^{year} - 1} \quad (26)$$

In which 'year' is the system service life and i is the interest rate.

5. Case study

A diagram of the power plant in the city of Qeshm is presented in Fig. 4. In Fig. 4 there are the hot exhaust heat and exhaust it through its upper HRSG. Also, in this figure, the potential points for utilization of steam from the power plant are shown. One of the points where it is possible to utilize heat is the low pressure steam for MED and second point is using steam for running a steam turbine. Energy hub located on the island of Qeshm is close to the Kuvei city. The demand for consumed water (kg/s) for each hour during the year for Kuvei is determined which should be supplied by the energy hub. Its water demand to supply its 4243 population is 9.8 kg/s. Also, the consumption of electricity (kW) for each hour during the year is 1220 kW. Since the variances in consumption at various hours of the year are insignificant in relation to the consumption level, the average annual consumption for all hours can be considered. Also, the distance between the power plant and the city of Dargahan with 14525 population is approximately 1.9 km, which will allow the transfer and sales of excess water to the city.

6. Optimization

GA (Evolution) is an algorithm based on repetition. The strategy of this algorithm is to apply a random search to determine an optimal solution. In principle, the simple method of biological evolution is to emulate the evolutionary characteristics of a population of individuals in which the individual consists of decision variables values for a potential optimized solution.

Table 3. Values of economic parameters [53, 54, 55]

Economic parameters	Unit	Value
Interest rate (i)	%	10
Operation years (n)	Year	20
Operation hours in a year (N)	Hour	8000
Cost of fuel	$/m^3	0.15
Electricity sales price	$/kWh	0.015
Electricity purchase price	$/kWh	0.045
Heating cost	$/kWh	0.001
Desalinated water cost	$/m^3	0.002
CO_2 emission factor (ψ_{em})	$/kg $_{CO2}$	0.02086

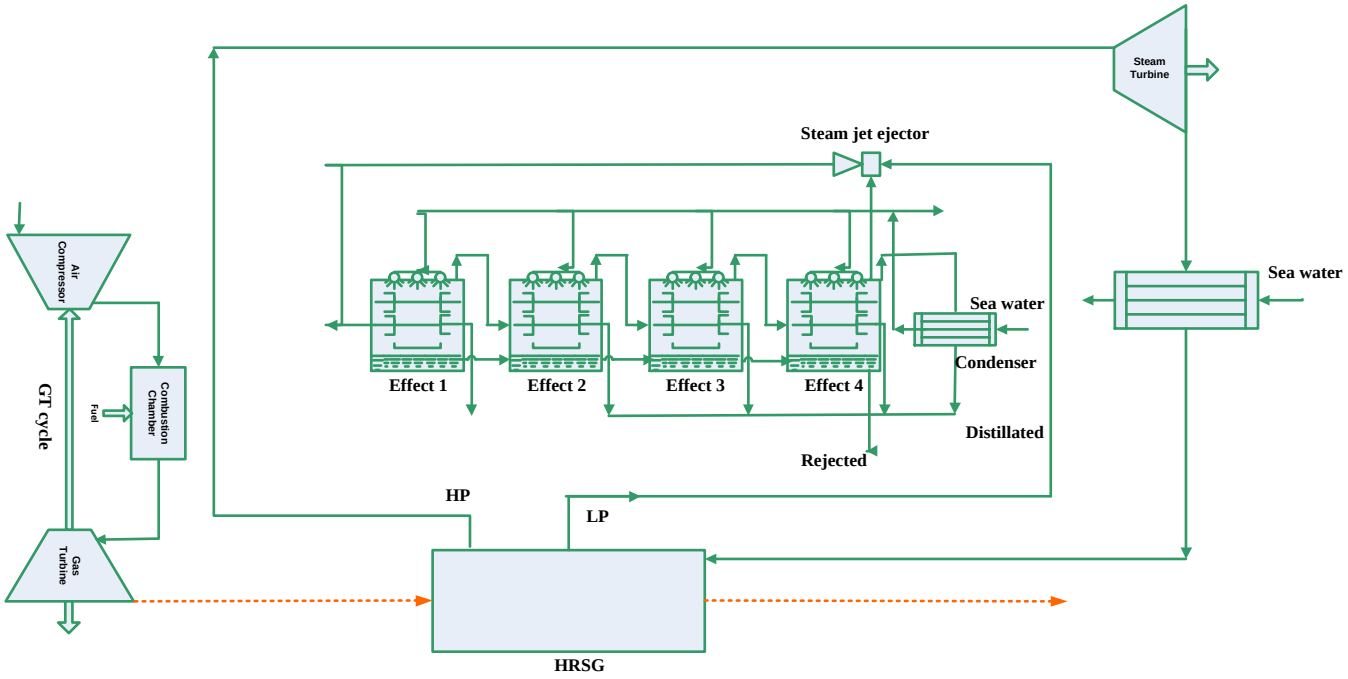

Fig. 4. Schematic of heat utilization potential in Qeshm power plant

The decision variables and optimization variables are given in Table 4. The objective functions of this optimization are Eq. (18) and Eq. (25) which determine the hub's exergy efficiency and economic parameter, respectively.

A decision making process should be employed to select a single optimal point from the present points on the Pareto front. Such process is typically based on engineering experiences where the importance of every decision making objective is highlighted. An assumed point taking the role of an ideal point is usually used to determine the final decision making process. When two objective functions are individually optimized whilst disregarding other objective functions, the compositions of these values symbolizes the ideal point or ideal objective point. Figure 5 presents the usual Pareto front in addition to the ideal point to maximize the first objective whilst minimizing the second objective. It is evident that it is not possible to achieve both objectives at optimal points concurrently. The closest Pareto frontier point to the ideal point may be chosen as the final optimal solution because the ideal point is not a solution that is placed on the Pareto frontier.

Table 4. Design parameters and their range of variation for the optimization procedure

	Parameter	Lower bound	Upper bound
CHP Power dispatch factor	v_{CHP} (-)	0	1
MED Water dispatch factor	v_{MED} (-)	0	1
Boiler Heat dispatch factor	v_{Boiler} (-)	0	1
Steam Turbine Power dispatch factor	v_{ST} (-)	0	1
RO Water dispatch factor	v_{RO} (-)	0	1
Water recovery rate (RO)	R_{RO} (%)	0.3	0.85
Hot water inlet temperature (MED)	T_{hot} (°C)	60	74
Hot water flow rate (MED)	M_{hot} ($L.s^{-1}$)	7	14
Power consumption per Water Desalinated (RO)	EW_{RO}(kJ/kg)	0.1	8
Maximum Heat Produced by Boiler	$Q_{max,Boiler}$ (kW)	100	3000

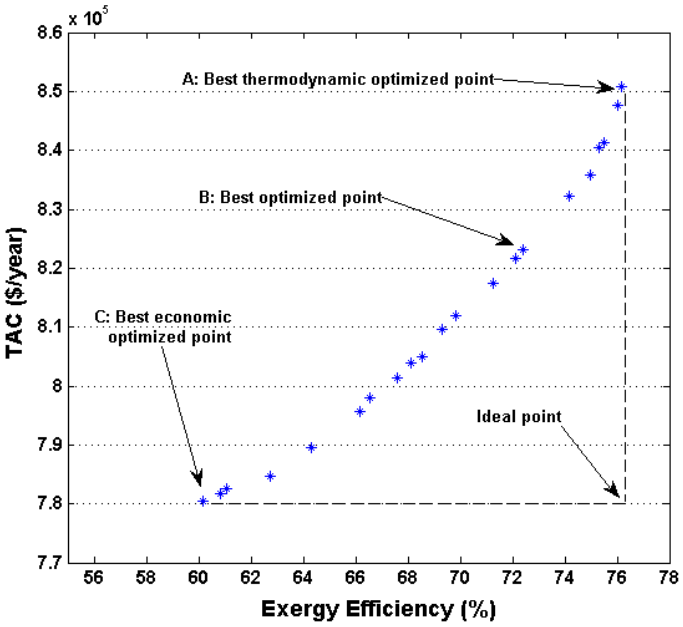

Fig. 5. Pareto optimal front for energy hub

Prior to this, the objectives are non-dimensionalized. LINMAP, linear programming techniques for multidimensional preferences analysis method is implemented to non-dimensionalize the objectives in this paper by employing the following equation [52]

$$F_{ij}^{n} = \frac{F_{ij}}{\sqrt[2]{\sum_{i=1}^{m}(F_{ij})^2}} \quad (27)$$

Such that i is the index for each Pareto front point, j is each objective's index and m displays the Pareto front's number of points. Hence, the distance for each Pareto front point from the ideal point is attained [52]:

$$d_i = \sqrt{\sum_{j=1}^{2}(F_{ij}^{n} - F_{ideal,j}^{n})^2} \quad (28)$$

Such that ideal is ideal objective function index. Thus, the value of distance for each Pareto frontier point is derived via the equation stated above and optimal point leading to minimum d is chosen as final optimal solution.

According to [43], some of the essential features of genetic algorithms optimization are:

(1) The generalization of the formulation.
(2) Looking for global optimal points, Robustness, in the sense of avoiding local optima.
(3) The ability of using multiple objectives.
(4) Computational efficiency decision variables.

7. Results

The Pareto curve is derived from two-objective optimization, and in order to achieve optimal decision variables and optimal objective function values, the two-objective functions will be TAC and exergy efficiency. Figure 5 shows the optimum Pareto front results for two objective functions. The acquired results show that two chosen objective functions i.e. energy efficiency and TAC differ in the optimal state. Attempts to enhance energy efficiency will increase TAC in both cases and vice versa. The confliction trend in the optimal state should be highlighted via multi-objective optimization. Increases in energy efficiency increases optimal TAC with the increment slope significantly increasing for maximum energy efficiency. Thus, the energy hub is not economically viable for maximum energy efficiency. The developer should choose the final optimal point according to the significance of each objective. Additionally, the optimum Pareto point is influenced by

optimal results acquired in the energy hub. Table 4 lists ten design factors i.e. decision variables along with relevant variation ranges in order to maximize energy efficiency value while minimizing TAC.

A decision making process is implemented to select the final solution from optimal Pareto front points. This process is conducted on the basis of the significance of every objective for the decision makers and engineering experiences and. Fig. 5 shows that at design point A (76.15%) there is maximum exergy efficiency exists and the TAC is highest at this point. Furthermore, at design point C, the minimum TAC is achieved (780514.7 $/year) along with the lowest exergy efficiency value (60.16%). The optimal exergy efficiency state as a single objective function is at design point A. The optimal condition where TAC is a single objective function is at design point C. Table 5 lists the optimal values for two objectives regarding five usual points from A-C (Pareto optimal fronts) for the input values stated in Table 6. Also, Table 6 shows that, moving from point A to point C, the v_{MED} value change approximately 0.18, which indicates a decrease in annual costs and a decline in exergy efficiency for the use of MED desalinating water.

Also, the use of a steam turbine to generate electricity and RO for water production remained the TAC and exergy efficiency constant. Since the city of Kuvei that is located in the vicinity of the power plant, has a specific population, as a result, the highest demand for energy carriers and heat is limited; resulting in the maximum purchases of electricity through a hub of 348 kW and maximum heat was sold to 412 kW. In the energy hub, urban water demand is a considered as the demand for energy hubs. Results indicate that due to the high costs of water transfer and the distance from the nearest city (Dargahan) to the power plant, there are no water sales outside the hub. Upon optimization and using the energy hub concept, the water purchased from the grid has dropped from 9.8 kg/s to 4.72 kg/s, indicating that part of the water is produced in the hub and utilized in the adjacent city (5.08 kg/s). Also, the energy hub is self-sustained in electricity maintenance, with the exception of the remaining 874 kW supplied by the GT and steam turbine. Also, in order to supply the NG required by the GT and boiler, 0.038 kg/s is consumed in the hub.

Another factor in reducing TAC can be accredited to the utilization of gas turbine. One of the features of this apparatus is its electricity and heat supply based on an initial production cost. Therefore, the genetic algorithm increases the role of this system in the energy hub leading to a reduction in the installation costs pertaining to other equipment such as a boiler.

As shown in Fig. 6, it is evident that energy efficiency increases with T_{hot} as expected. Considering the impact of m_{hot} on energy efficiency, it is clear that energy efficiency slightly decreases for Low m_{hot} (from 12 L/s to 8 L/s) while increasing considerably (approximately 1.2%) for smaller m_{hot}. Such progressive decreases may

Table 6. The optimum values of design parameters for optimum selected points A–C in Pareto optimum front.

Parameter	With Waste heat recovery		
	A	B (Best Point)	C
v_{CHP} (-)	0.99	0.92	0.93
v_{MED} (-)	0.01	0.04	0.19
v_{Boiler} (-)	0.20	0.72	0.67
v_{ST} (-)	0.30	0.31	0.31
v_{RO} (-)	0.86	0.92	0.92
R_{RO} (%)	0.38	0.38	0.40
T_{hot} (°C)	60.61	65.60	63.96
M_{hot} ($L.s^{-1}$)	12.59	12.85	12.47
EW_{RO}(kJ/(kg))	0.11	0.11	0.11
$Q_{max,Boiler}$ (kW)	2284.83	2108.43	2111.31

be because of the evaporative process via the tube bundle that is nearer to its hot water temperature design value (11.54 L/s). Due to the increases in thermal energy used which is greater than the distillate production, an energy efficiency reduction is experienced by Q_{MED}. Also, by growing the rate of T_{hot} (from 60 °C to 74 °C), the exergy efficiency increases by 1.5%.

Figure 7 shows v_{RO}, v_{MED} variations in terms of TAC. In this figure, with v_{MED} variations from 0 to 1, TAC increase by an average of 30.1%. Also, v_{RO} variations from 0 to 1 will increase TAC by an average of 25% and up from 749362 $/year. By increasing the allocated share of fresh water production to the RO system, it is evident that TAC costs have increased. In order to produce more water, the RO system requires higher water pressure from the intake water supply as well as higher water pressure. By allocating more energy to this component, the water pressure will increase.

In the current system, the following resources are used to meet the demand of the consumption section. Electricity supply from the national grid (conventional centralized power plants on the island), fresh water produced from the RO system and heating based on current heat generators is dispersed for each consumer. Also, since the systems are designed to just meet the demands of consumers, purchases and sales with the grid are not considered. Table 7 presents the results of the basic parameters of the hub both in an optimal state and current state. In the optimal scenario, by recovery waste heat from the gas turbine, heating, power and water generation in addition to optimizing energy flows and capacity of utilized equipment, fuel consumption will be reduced by over half whilst exergy efficiency will increase by 34.31%. Also, Co_2 emission will drop by 471 ton/year and TAC will decrease by about 257904 $/year.

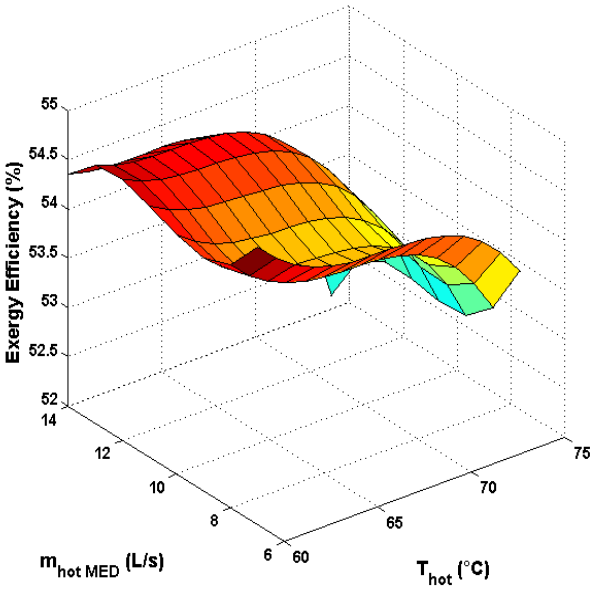

Fig. 6. The rate of exergy efficiency in energy hub at hot water flow rate and hot water temperature

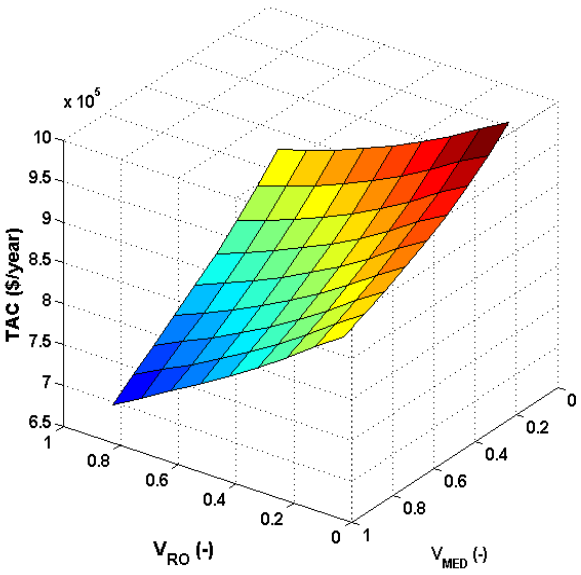

Fig. 7. The rate of TAC in energy hub versus dispatch factors of MED and RO

Table 7. Comparison of results between basic parameters of the optimal scenario and current system on Qeshm Island

Parameter	Current system	Optimized System
CO_2 Emission (kg_{CO2}/year)	7945600	5235053
η_{ex} (%)	38.1	72.41
TAC ($/year)	1081060	823155.7

According to the reference [56], 443 grams of carbon dioxide are produced, for every one kWh of power production by combine cycle power plants. As the amount of power consumption in energy hub side is 1221 kW, about 7035.4 tons of carbon dioxide will be produced annually. Regarding power production at the power plant which is equivalent to the reduced carbon dioxide for the recovered waste heat, carbon dioxide is declined by 75%. In the case of energy hub, the CO_2 gas produced is considered based on electricity, and water demand from the grid. The demand for water is 9.8 kg/s which produce 910 tons of CO_2 per year. With the energy hub, upon optimization and heat recovery from gas turbine, the consumption of NG is 0.038 kg/s equivalent to 3649 tons of CO_2 per year for power generation in GT which is the main CO_2 producer when using the energy hub. While, the primary energy of desalination systems is captured from the power and heat generated within the energy hub, it is therefore considered to be equivalent to the change in carbon dioxide emissions in the primary energy changes, and thus the carbon dioxide generated by the production of water is not taken into account. Considering all energy carriers before and after optimization, the environmental impact of producing 7.945 thousand tons of CO_2 per year has been reduced to 7.474 thousand tons of CO_2 per year (Fig. 8).

Figure 9 shows the sensitivity analysis conducted on key factors such as water price, heating and electricity. The results from this analysis highlighted the energy carrier with negative slope that may be supplied with other sources and acquired with positive slope.

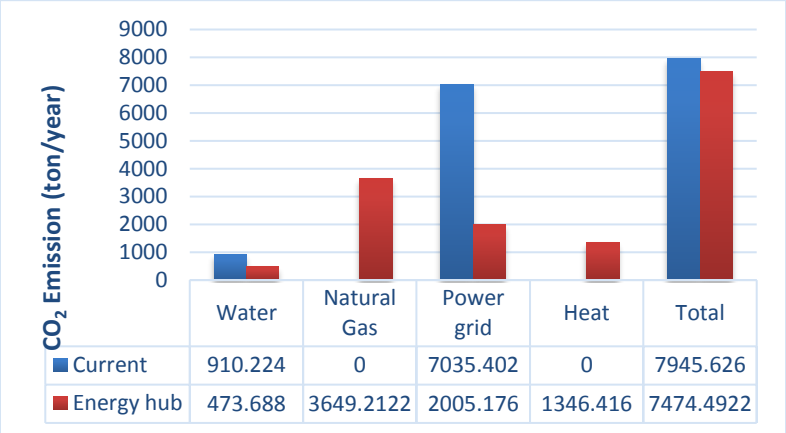

Fig. 8. Variation of CO_2 emissions (kg_{CO2}/year) and energy carrier with energy hub and current system

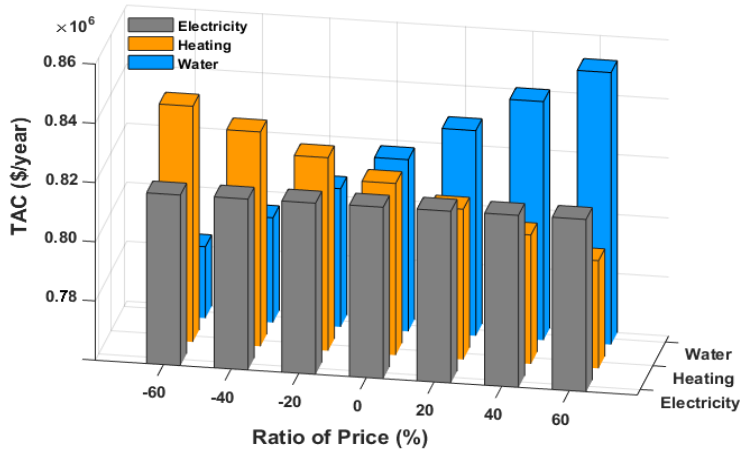

Fig. 9. Variation of TAC versus ratio of price and energy carrier in energy hub

The achieved results show that when water selling price increases, the TAC is significantly raised with constantly varying costs. The optimal system tends to function on the basis of water sales. The TAC will increase as much as 6.6% because of the raise in water price ration. In addition, Fig. 9 depicts that with higher heating sales price ration from -60% to 60%, overall system TAC will be reduced by 4%. Based on the data shown in Fig. 9, it is evident that an increase in electricity price has less influence on TAC in comparison to other energy carriers.

The impact of m_f validation on the distillate production and GOR are shown in Table 8. Moreover, the measurement errors and numerical results are presented in this table. These measurement errors originate from discrepancies between the empirical formula and empirical values in reference [38]. Moreover, the presented empirical model in the section 2.3 stemming from the extensive empirical results has been compared with reference [47] (Fig.10). This comparison was conducted under conditions where the values of m_f and T_f were within the acceptable range of the empirical model. This comparison shows that the empirical model has minor differences with the numerical results and the relevant errors are acceptable in terms of empirical model application.

In the single-objective optimization of an energy hub with TAC objective function, the genetic algorithm and PSO methods were adopted with close results. The value for TAC was 793,393 $/year upon convergence in single-objective optimization of the genetic algorithm and the value for PSO was 798,359 $/year. However, in two-objective optimization the value for TAC was 823,155 $/year. Such increase is due to the simultaneous effect of TAC and exergy efficiency (Fig. 11).

Table 8.Average values of empirical results of GOR and distillate production with measurement errors

Hot water inlet temperature (°C)	Feed water flow rate (m3/h)	Distillate production (m3/h)	GOR
74	5	2.49±0.07	8.89±1.08
74	6	2.65±0.10	9.27±1.41
74	7	2.83±0.08	9.39±1.03
74	8	2.95±0.07	9.42±0.91
74	9	3.00±0.08	9.39±1.03
72	5	2.41±0.07	9.20±1.06
72	6	2.57±0.07	9.40±1.01
72	7	2.72±0.08	9.54±1.18
72	8	2.79±0.08	9.65±1.16
72	9	2.83±0.08	9.54±1.12
70	5	2.33±0.08	9.48±1.31
70	6	2.50±0.06	9.80±1.02
70	7	2.65±0.08	9.87±1.18
70	8	2.76±0.08	10.05±1.23
70	9	2.75±0.07	9.65±1.00
68	5	2.30±0.11	10.30±2.00
68	6	2.46±0.11	10.60±1.89
68	7	2.63±0.08	10.78±1.25
68	8	2.73±0.09	11.10±1.50
68	9	2.73±0.08	10.10±1.23

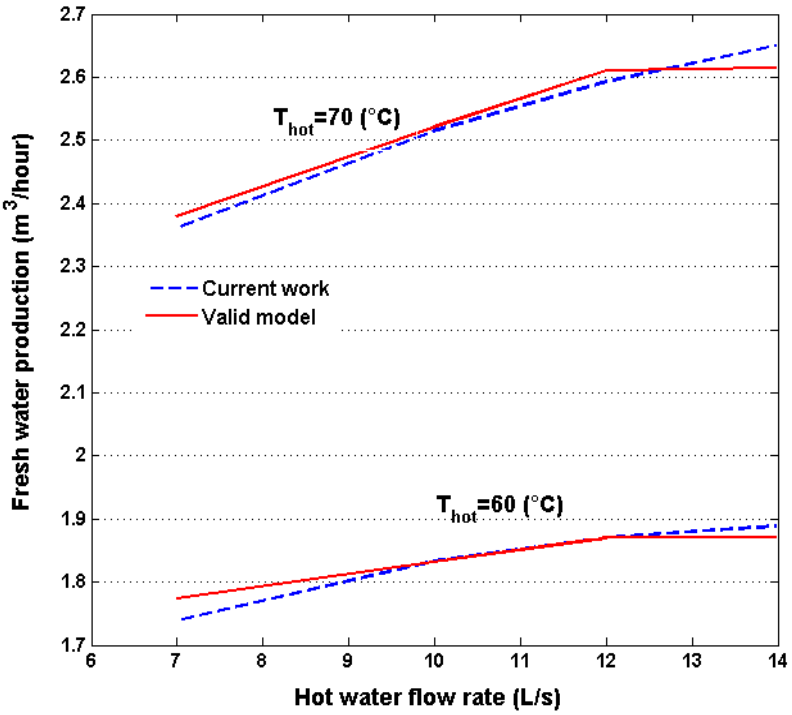

Fig.10. MED model validation with a valid model in various hot water inlet temperatures

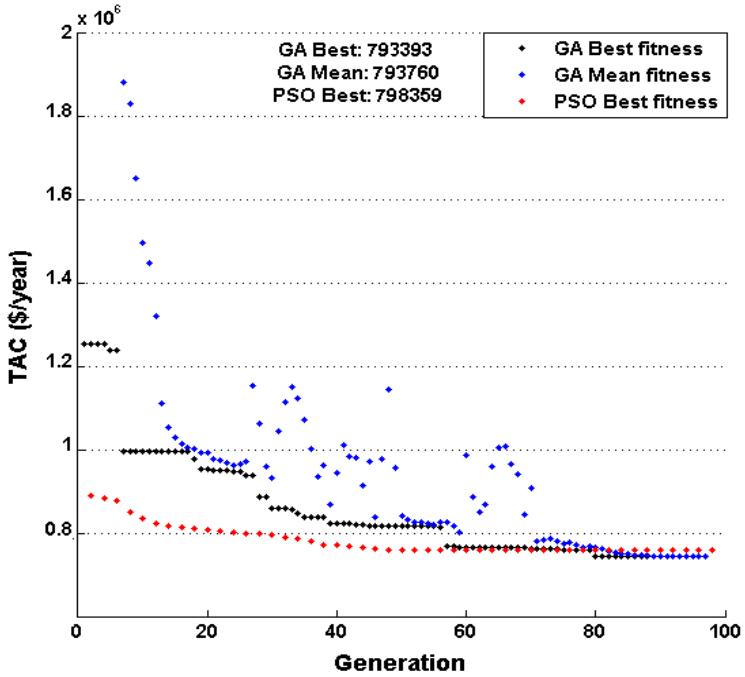

Fig.11. Comparison of single-objective optimization using GA and PSO for TAC objective function

8. Conclusions

In this paper the TAC for the energy hub and energy efficiency was optimized by taking into account the waste heat recovery from the power plant as an energy hub. The GA was employed to determine optimal values regarding ten design factors to maximize two proposed objective functions defined as energy efficiency and TAC. Concurrent selection of maximum heat produced by boiler, power consumption per water desalinated, MED hot water flow rate, MED hot water inlet temperature, and water recovery rate took place with dispatch factors for RO and MED water production, steam turbine power, boiler heat, MED water, and CHP power. The acquired research results are presented below:

- After optimization and comparing the beam curve, it was found that upon applying the energy hub and energy recovery, the exergy efficiency and TAC increased by 34.31% and decreased by 23.8% respectively.
- CO_2 emissions reduced from 7945.6 tons per year to 7474.49 tons per year upon utilizing the energy hub concept.
- The lower the share of water production, the higher the price of water per cubic meter

References

[1] Stewart B, Hoang M, Zarzo D, Olewniak F, Campos E, Bolto B, Barron O. Desalination techniques: A review of the opportunities for desalination in agriculture. Desalination 2015; 364:2–16.

[2] Lattemann S, Kennedy M.D, Schippers J.C, Amy G. Sustainable water for the future: water recycling versus desalination chapter 2 global desalination situation, Sustain. Water Future 2010; 2:7–39.

[3] Lattemann S, Kennedy M.D, Shippers J.C, Amy G. Sustainability Science and Engineering, Elsevier B.V., 2010.

[4] GWI, IDA, Desalination Yearbook 2016–2017, Water Desalination Report. Global Water Intelligence 2016.

[5] Voutchkov N. Energy use for membrane seawater desalination – current status and trends. Desalination 2018; 431:2-14.

[6] AcuaMed, La desalación en España. Sostenibilidad para zonas vulnerables (Desalination in Spain. Sustainability for vulnerable areas), Ministry of Environment, Rural and Marine. Spain Government, 2011.

[7] Shalaby S.M. Reverse osmosis desalination powered by photovoltaic and solar Rankine cycle power systems: A review. Renewable and Sustainable Energy Reviews 2017; 73:789–797.

[8] Choon Ng K, Shahzad M. Wakil. Sustainable desalination using ocean thermocline energy. Renewable and Sustainable Energy Reviews 2018; 82:240–246.

[9] Pouyfaucona A. Buenaventura, García-Rodríguez L. Solar thermal-powered desalination: A viable solution for a potential market. Desalination 2018; 435:60-69.

[10] Mokhtari H, Ahmadisedigh H, Ebrahimi I. Comparative 4E analysis for solar desalinated water production by utilizing organic fluid and water. Desalination 2016; 377:108–122.

[11] Salcedo R, Antipova E, Boer D, Jiménez L, Guillén-Gosálbez G, Multi-objective optimization of solar Rankine cycles coupled with RO desalination considering economic and life cycle environmental concerns. Desalination 2012; 286:358–371.

[12] Sharon H, Reddy K.S. A review of solar energy driven desalination technologies. Renewable and Sustainable Energy Reviews 2015; 41:1080–1118.

[13] Roger J. Francey, Cathy M. Trudinger, Marcel van der Schoot, Rachel M. Law, Paul B. Krummel, Ray L. Langenfelds, L. Paul Steele, Colin E. Allison, Ann R. Stavert, Robert J. Andres, Christian Rödenbeck. Atmospheric verification of anthropogenic CO2 emission trends. Nature Climate Change 2013; 3:520–524.

[14] Peters GP, Andrew RM, Boden T, Canadell JG, Ciais P, Quéré C. Le, Marland G, Raupach MR, Wilson C, the

challenge to keep global warming below 2 °C. Nature Climate Change 2013; 3:4–6.

[15] Kabeel AE, El-Said Emad MS. Technological aspects of advancement in low-capacity solar thermal desalination units. International Journal of Sustainable Energy 2013; 32: 315-332.

[16] Kabeel AE, El-Said Emad MS. Economic analysis of a small-scale hybrid air HDH-SSF (humidification and dehumidification water flashing evaporation) desalination plant. Energy 2013; 53:306-311.

[17] Brahman F, Honarmand M, Jadid S, Optimal electrical and thermal energy management of a residentialenergy hub, integrating demand response and energy storage system. Energy and Buildings 2015; 90:65–75.

[18] Mohammadi M, Noorollahi Y, Mohammadi-ivatloo B, Hosseinzadeh M, Yousefi H, Torabzadeh Khorasani S. Optimal management of energy hubs and smart energy hubs – A review. Renewable and Sustainable Energy Reviews 2018; 89:33–50.

[19] AlRafea K, Fowler M, Elkamel A, Hajimiragha A. Integration of renewable energy sources into combined cycle power plants through electrolysis generated hydrogen in a new designed energy hub. International journal of hydrogen energy 2016; 41:16718-16728.

[20] Togawa T, Fujita T, Dong L, Fujii M, Ooba M. Feasibility assessment of the use of power plant-sourced waste heat for plant factory heating considering spatial configuration. Journal of Cleaner Production 2014; 81:60-69.

[21] Amiri A, Vaseghi M.R. Waste Heat Recovery Power Generation, Systems for Cement Production Process. IEEE Transactions on Industry Applications 2015; 51:13 – 19.

[22] Kabir G, Abubakar A.I, El-Nafaty U.A. Energy audit and conservation opportunities for pyroprocessing unit of a typical dry process cement plant. Energy 2010; 35:1237–1243.

[23] Renewable Energy Organization of Iran. www.satba.gov.ir. (Access time: 2017)

[24] Madlool N.A, Saidur R, Hossain M.S, Rahim N.A. A critical review on energy use and savings in the cement industries, Renew. Sustain. Energy Rev. 2011; 15:2042–2060.

[25] Salimi M, Amidpour M. Investigating the integration of desalination units into cogeneration systems utilizing R-curve tool. Desalination 2017; 419:49-59.

[26] Chiranjeevi C, Srinivas T. Augmented desalination with cooling integration Dessalement augmenté avec refroidissement. International Journal of Refrigeration 2017; 80:106-119.

[27] Astolfi M, Mazzola S, Macchi P. Silva Ennio. A synergic integration of desalination and solar energy systems in stand-alone microgrids. Desalination 2017; 419:169-180.

[28] Mokhtari H, Sepahvand M, fasihfar A. Thermoeconomic and exergy analysis in using hybrid systems (GT+MED+RO) for desalination of brackish water in Persian Gulf. Desalination 2016; 399:1-15.

[29] Shahzad M. W, Burhan M, Ng K.C. Pushing desalination recovery to the maximum limit: Membrane and thermal processes
integration. Desalination 2017; 416:54-64.

[30] Azhar M. Shuja, G. Rizvi, Dincer I. Integration of renewable energy based multigeneration system with desalination. Desalination 2017; 404:72-78.

[31] Nemati A, Sadeghi M, Yari M. Exergoeconomic analysis and multi-objective optimization of a marine engine waste heat driven RO desalination system integrated with an organic Rankine cycle using zeotropic working fluid, Desalination. 2017; 422:113-123.

[32] Reynolds J, Ahmad M. W, Rezgui Y, Hippolyte J. Operational supply and demand optimization of a multi-vector district energy system using artificial

neural networks and a genetic algorithm. Applied Energy 2019; 235:699–713.
[33] Moeini-Aghtaie M, Fotuhi-Firuzabad M. Multiagent Genetic Algorithm: An Online Probabilistic View on Economic Dispatch of Energy Hubs Constrained by Wind Availability. IEEE Transactions on sustainable energy 2014; 5:699–708.
[34] Ko M. J, Kim Y. Sh, Chung M. H, Jeon H. Ch. Multi-Objective Optimization Design for a Hybrid Energy System Using the Genetic Algorithm. Energies 2015; 8:2924-2949.
[35] Kampouropoulose K. Multi-objective optimization of an energy hub using artificial intelligence, A thesis for the degree of Doctor of Philosophy in Electrical Engineering, Universitat Politècnica de Catalunya, Barcelona, Catalonia, Spain, 2018.
[36] Mohammadi S, Moradi-Dalvand M, Ghasemi H, Ghazizadeh M.S. Optimal Design of Multicarrier Energy Systems Considering Reliability Constraints. IEEE Transaction on Power Delivery 2015; 30:878-886.
[37] Geidl M, Koeppel G, Favre-Perrod P, Klöckl B .The Energy Hub – A Powerful Concept for Future Energy Systems. Third Annual Carnegie Mellon Conference on the Electricity Industry 2007:13 – 14.
[38] Chorak A, Palenzuela P, Alarcón-Padilla D.C, Abdellah A. B. Experimental characterization of a multi-effect distillation system coupled to a flat plate solar collector field: empirical correlations. Applied Thermal Engineering 2017; 120:298-313.
[39] Water & Process Solutions, FILMTEC™ Reverse Osmosis Membranes Technical, Dow Water & Process Solutions - The Dow Chemical Company. (Access time: 2011)
[40] Guideline for drinking Water Quality, Fourth edition incorporation the first addendum, World Health Organization. 2017.
[41] Asgari S, Noorpoor A.R, Boyaghchi F.A. Parametric assessment and multi-objective optimization of an internal auto-cascade refrigeration cycle based on advanced exergy and exergoeconomic concepts. Energy 2017; 125:576-590.
[42] Rosen MA, Dincer I, Kanoglu M. Role of exergy in increasing efficiency and sustainability and reducing environmental impact. Energy Policy 2008; 36:128-137.
[43] Ameri M, Mokhtari H, Mostafavi Sani M. 4E analyses and multi-objective optimization of different fuels application for a large combined cycle power plant. Energy 2018; 156:371-386.
[44] Boyaghchi F. A, Chavoshi M, Sabeti V. Multi-generation system incorporated with PEM electrolyzer and dual ORC based on biomass gasification waste heat recovery: Exergetic, economic and environmental impact optimizations. Energy 2018; 145:38-51.
[45] Sharqawy Mostafa H, Lienhard John H, Zubair Syed M. On exergy calculations of seawater with applications in desalination systems, International Journal of Thermal Sciences 2011;50:187-196.
[46] BarzegarAvval H, Ahmadi P, Ghaffarizadeh A.R, Saidi M.H. Thermo-economic-environmental multiobjective optimization of a gas turbine power plant with preheater using evolutionary algorithm, Int. J. Energy Res 2011; 35: 389–403.
[47] Ghasemi A, Heidarnejad P, Noorpoor A.R. A novel Solar-Biomass Based Multi-Generation Energy System Including Water Desalination and Liquefaction of Natural Gas System: Thermodynamic and Thermoeconomic optimization. Journal of Cleaner Production 2018; 196:424-437.
[48] Piacentino A. Application of advanced thermodynamics, thermoeconomics and exergy costing to a Multiple Effect Distillation plant: In-depth analysis of cost formation process. desalination 2015; 371:88–103.
[49] Hajabdollahi H. Investigating the effects of load demands on selection of optimum CCHP-ORC plant. Applied Thermal Engineering 2015; 87:547-558

[50] Breeze P. The Cost of Power Generation The current and future competitiveness of renewable and traditional technologies. 2010.

[51] Sanaye S, Khakpaay N. Simultaneous use of MRM (maximum rectangle method) and optimization methods in determining nominal capacity of gas engines in CCHP (combined cooling, heating and power) systems. Energy 2014;72:145-158.

[52] Boyaghchi F. A, Chavoshi M. Monthly assessments of exergetic, economic and environmental criteria and optimization of a solar micro-CCHP based on DORC. Solar Energy 2018; 166: 351-370.

[53] Web Site of Iranian Ministry of Energy, www.moe.gov.ir. (Access time: 2018)

[54] Hajabdollahi H, Ganjehkaviri A, Nazri Mohd Jaafar M. Assessment of new operational strategy in optimization of CCHP plant or different climates using evolutionary algorithms. Applied Thermal Engineering 2015; 75:468-480.

[55] Mabrouk A, Nafey A.S, Fath H.E.S. Thermoeconomic analysis of some existing desalination processes. Desalination 2007; 205:354–373.

[56] United States Environmental Protection Agency, www.epa.gov. (Access time:2018)